2017 IEEE World Haptics Conference (WHC)
Fürstenfeldbruck (Munich), Germany
6–9 June 2017

The Application of Tactile, Audible, and Ultrasonic Forces to Human Fingertips Using Broadband Electroadhesion

Craig D. Shultz, Michael A. Peshkin, and J. Edward Colgate

***Abstract*— We report an approach to controlling friction forces on sliding human fingertips in order to produce simultaneous vibrations across an exceedingly broad range of tactile, audible, and ultrasonic frequencies. Vibrations in the skin can be felt directly by the fingertip, and vibrations in the air can be heard emanating from the proximity of the finger.**

We introduce and detail an experimental apparatus capable of recording friction forces up to a frequency of 6 kHz, and describe a custom designed electroadhesive amplifier and system with a flat current to force magnitude response throughout this entire measurement range. Recordings with a MEMS microphone confirm the existence of ultrasonic forces applied to the finger and further reveal the ultra wideband capability of broadband electroadhesion. Implications for the design of surface haptic and general audio-haptic displays are discussed.

I. Introduction

Surface haptic displays aim to apply programmable forces to bare fingertips on flat surfaces. Geared towards enriching the user experience of touchscreen devices, these displays show promise of being seamlessly incorporated into everyday human computer interactions. One class of surface haptic device which has received great interest are variable friction displays, so-called as they modulate the inherent frictional forces encountered by a finger sliding on a flat surface.

When operated at steady state, variable friction displays are able to stop a sliding finger in place or reduce friction to a negligible level. These effects are achieved by applying additional Coulombic force, which increases friction [1][2][3], or by altering the finger/surface interface via low amplitude, ultrasonic oscillations [4][5], which decreases friction. These effects can also be combined for greater dynamic range [6].

While the quasi-static behavior of these displays has been the primary subject of research for some time by our lab and others, more recent applications utilize increasingly rapid modulation of friction. This transition towards dynamic actuation stems from the fact that, at the time of this work, all known variable friction displays actuate the entire fingerpad in spatial synchrony, i.e. the entire fingerpad is activated at once. This synchrony offers impoverished information to slowly adapting type I tactile afferents (Merkel's discs), which are sensitive to spatial distributions of strain energy across the fingerpad. In contrast, dynamic modulation of friction is thought to offer rich information for both fast adapting type I (Messiner's Corpuscles) and type II (Pacinian Corpuscles) tactile afferents, which are most sensitive to transient and broadband vibrations in the range of approximately 10-1000 Hz [7][8]. Properly actuating the fingertip at these high frequencies may by critical to new surface haptic applications such as virtual texture display [9][10].

A principal goal of this research is to develop an approach to variable friction surface haptics that is sufficiently broadband to offer rich excitation of fast adapting type I and II afferents. In this paper we demonstrate that not only is broadband tactile excitation possible, but the method developed may be easily extended to produce programmable audio emanating from a fingertip, adding a complementary sensory modality to the interaction experience.

C D Shultz, M A Peshkin, and J E Colgate are with the Mechanical Engineering Department, Northwestern University, Evanston, IL, 60208, USA. craigdshultz {@u.northwestern.edu}, peshkin, colgate {@northwestern.edu}

978-1-5090-1425-5/17/$31.00 ©2017 IEEE

II. Background

A. Wide-Bandwidth Variable Friction

The quasi-static behavior of variable friction devices has been previously addressed in the literature and will be briefly addressed in this work. An emerging area of study, however, is devoted to the question of total system bandwidth.

In 2014, Meyer et al. [11] performed initial bandwidth measurements on electroadhesive and ultrasonic variable friction devices, showing overall magnitude and transient responses. Both methods exhibited roll-offs in force starting around 130 Hz. Beyond this frequency, the ultrasonic device continued to show additional force attenuation, while the electroadhesive device appeared to flatten out to until the end of their 1 kHz measurement range. The authors proposed a second-order resonant mechanical model to explain the attenuation of the ultrasonic device, but offered limited characterization of the electroadhesive device. They only suggested that electroadhesive devices are more responsive than their ultrasonic counterparts, presumably due to their solid state nature. A conclusion was that electroadhesive surfaces showed promise for wide-bandwidth force display.

Followup work showed that the limited bandwidth of the ultrasonic device could be mostly corrected for by using a compensation filter and high performance piezo amplifier, capable of driving the piezos at an increasing voltage with increasing modulation frequency [12]. These techniques led to improved high frequency performance at the cost of added complexity and power consumption. This inherent tradeoff between bandwidth and power consumption in ultrasonic devices was also commented on by Wiertlewski et al. [13].

Similar transient step response measurements were made on ultrasonic and electroadhesive devices by Vezzoli et al. [6]. Their measurements supported the conclusion that ultrasonic devices are limited by resonance. They also suggested that electroadhesive devices would only be limited by

amplifier bandwidth, and a high-bandwidth amplifier should yield high-bandwidth forces. This work employs such an amplifier, and details the manner of its application.

B. Electroadhesion: A Physical Phenomenon

The term electroadhesion refers to the generalized physical principle of increased adhesion between two contacting surfaces brought about by the application of Coulombic attraction across their interface [14]. While the name is drawn from the work of early 20th century scientists studying the effect [3], the earliest known observations of electroadhesion occurred in the late 1800s, predating, and in fact precipitating, the controversial invention of the telephone in 1876 [15]. Discovered in 1874 and detailed in a patent in 1875 by inventor Elisha Gray, the acoustic vibration induced by an electric current flowing through a finger sliding on a conductive acoustic body was used as an early example of how an electrical telegraph could be utilized to convey musical tones across a wire [16].

Gray's method of transduction, however, was usurped by more practical designs and seemingly neglected until its rediscovery, once again because of sliding fingers, by the Danish scientists Johnsen and Rahbek in the early 1920s [14]. Forgotten yet again, it was rediscovered and documented in the 1950s by Mallinckrodt running his finger across a poorly wired light socket [17].

The effect was first used for tactile display purposes in 1970 [18], and a subset of the effect garnered the name electrovibration in 1983 [19]. A later electrotactile display was made by Beebe et al. [20], and the first applications of the effect for visuo-tactile display were described by Linjama and Mäkinen [1], followed by Bau et al. [2]. The first systematic force measurements with human fingers were made by Meyer et al. [21]. This work was also the first known attempt to introduce high frequency amplitude modulation to generate a constant adhesion force that could be adjusted arbitrarily. This method of actuation differed from previous so-called electrovibration devices which utilized rectified electroadhesive force ripple, typically produced by applying single frequency voltage excitation to the finger.

All modern devices, however, still only produced force on the finger via polarized bound charge. In contrast, Shultz et al. [3] described and demonstrated the first modern usage of free charge to produce force, an effect sometimes named after Johnsen and Rahbek. This work also introduced an electrical impedance based force model to unite bound and free charge effects, and, in doing so, suggested electroadhesion as a general term to encompass all manners of Coulombic attraction based devices (a convention adopted here).

III. Methods and Apparatus

A. Rotational Tribometer

A custom rotational tribometer was constructed for wide-bandwidth friction force measurements. The device was built around a modified turntable (ST.150, Gibson Guitar Company, TN, USA) and DAQ (NI USB-6361, National Instruments, TX, USA), sampling at a rate of 250 kHz. The direct drive turntable maintains a constant rotational velocity via an internal controller and is monitored by reading the internal encoder. A general layout of the apparatus can be seen in Fig. 1.

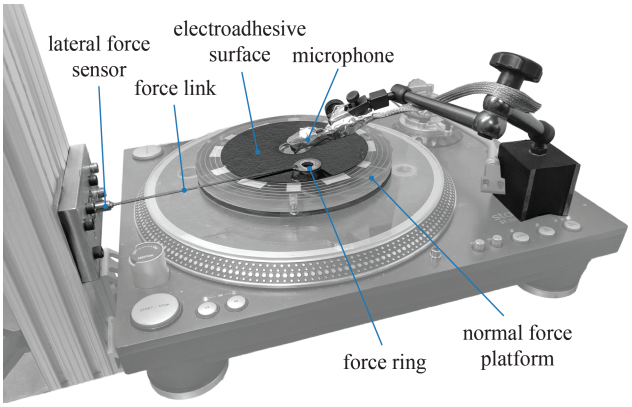

Fig. 1. Overview of rotational tribometer apparatus and recording instruments. The rotational slip ring, hand rest, and supporting frame have been temporarily removed for clarity.

Normal force applied by the finger was monitored using a custom force platform based on three piezoresistive force sensors (FSS1500NSR, Honeywell, MN, USA). The force signal was conveyed off of the platform using a rotational slip ring and displayed on a visual screen for user feedback.

Lateral force was measured using a piezoelectric force sensor and charge amplifier (9217A and 5010B, Kistler Instrumente AG, Winterthur, Switzerland) which was coupled to a patch of skin contacting the rotating plate via a carbon fiber link and a 0.5 mm thick FR4 fiberglass ring with 25 mm OD and 13 mm ID (also shown in Fig. 2a). A PTFE ring spacer, 0.5 mm thick with 25 mm OD and 24 mm ID, was affixed to the bottom of the fiberglass ring. This spacer ensures that any normal force not traveling though the contact patch has minimal effect on measured lateral force.

B. Electroadhesive Surface

The electroadhesive surface used was an aluminum disc, 150 mm in diameter and 1 mm in thickness, coated with a diamond like carbon (DLC) coating. The coating is 2-3 μm thick and goes by the trade-name BALINIT® DYLYN PRO. This coating was chosen due to its dielectric and frictional properties, as well as its overall thickness and robustness to wear. In particular, it shows good stability in friction force with fingertip sweat pore occlusion, allowing friction measurements that are consistent over large time scales.

C. Ultrasonic Microphone

Audio was recorded using a MEMS microphone (SPU0410LR5H-QB, Knowles Electronics, IL, USA). This microphone's frequency response is flat from 100-10,000 Hz, exhibits a broad resonance at 25 kHz, and reduced but still appreciable sensitivity far into the ultrasonic regime, allowing basic ultrasonic measurements to be made. The microphone was placed a few centimeters from the fingertip.

D. High Performance Current Controller

Current control is utilized in all experiments for two primary and related reasons: safety and uniformity of effect. Recommended current threshold levels outlined in [22] were adhered to for all experiments, and applied current remained below the limit of electrocutaneous stimulation.

A custom, high voltage compliant, transcondutance amplifier was constructed and characterized. The amplifier can source or sink up to 5 mA with a voltage compliance of $\pm$500 V. It is built around a high common mode voltage differential amplifier (AD8479, Analog Devices Inc, MA, USA) in a bootstrapped power supply configuration. Current is controlled via a 1 kΩ 0.1% shunt resistor in a modified Howland current source topology.

Current was supplied to the rotating surface via an electrical slip ring. When the surface is touched, current travels through the finger and exits the hand by way of a Ag/AgCl electrode applied to the user's palm. Another 1 kΩ 0.1% shunt resistor was used to measure return current from the electrode, and a custom 50:1 high impedance probe was used to measure total applied voltage. Redundant internal safety mechanisms limit the possible applied current to $<$10 mA.

Output impedance of the amplifier was measured to be on the order of 20 MΩ, limited only by the common mode rejection ratio (CMRR) of the differential amplifier. The amplifier bandwidth is limited by stray output capacitance to ground, and a capacitance compensation feedback circuit was utilized to mitigate this effect. With capacitance compensation, the measured -3 dB bandwidth into a typical load impedance was 45 kHz. Additionally, total harmonic distortion (THD) for applied current was measured to be less than 1% throughout this entire range.

IV. Modeling and Analysis

A. Lateral Impedance Model and Analysis

A representation of the lateral force measurement setup can be seen in Fig. 2a. The FR4 ring is glued to the perimeter of the skin contact patch using cyanoacrylate adhesive prior to measurements. This ring is intended to isolate the contact patch from the rest of the finger and bone. When linked to the force sensor, it serves to shunt the contact patch lateral stiffness to the bone with the much higher stiffness of the sensor, while adding minimal moving mass (seen in Fig. 2b).

The lateral impedance of an engaged fingertip to bone can be modeled by a linear spring-mass-damper system, with a damped natural resonance occurring around 250 Hz [23]. The equivalent stiffness of a typical fingertip skin patch is low ($\approx$ 1 N/mm), as is the moving mass ($\approx$ 0.1 g). The piezo force sensor used has a stiffness four orders of magnitude greater ($\approx$ 15000 N/mm) and a small moving mass ($<$ 1 g). The carbon fiber link and fiberglass ring were designed to achieve a high stiffness to weight ratio, so as to reduce their impact on the sensor's performance. The distributed mass and stiffness are lumped into m_{sense} and k_{sense}.

Averaged impulse responses of the force link/sensor are shown in Fig. 2c. These responses show a large compression

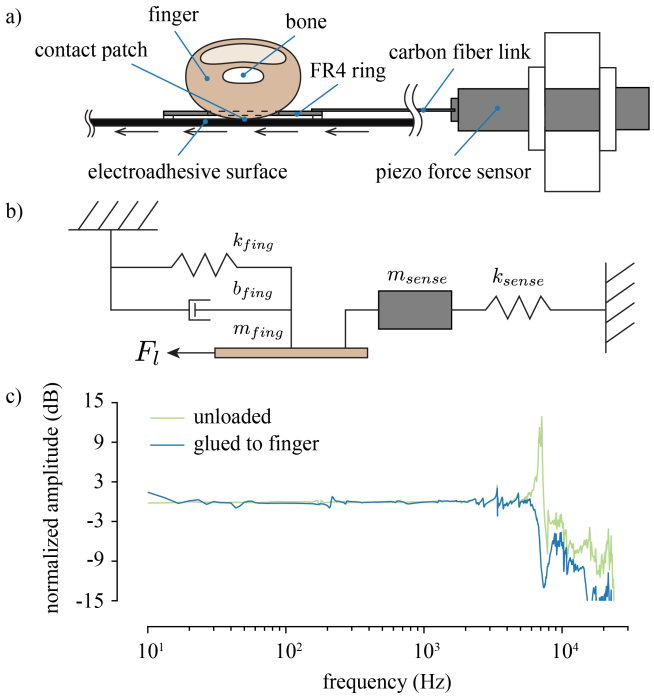

Fig. 2. a) Cross-section of a finger, glued to a FR4 ring, pressed against the rotating electroadhesive surface. The FR4 ring is affixed to a carbon fiber link and piezo force sensor. b) Lumped lateral impedance model showing the connection of the finger mass and force link/sensor. c) Normalized impulse response of a ball bearing pendulum striking the force link/sensor in axial compression. Each trace represents the mean of 20 trials.

mode resonance at approximately 7 kHz, which is damped, but not shifted in frequency, when the lead author's finger is glued to the force ring. This analysis implies that, below the resonance of the force link/sensor, the measured lateral force represents the applied lateral force at the perimeter of the skin contact patch.

B. Friction Model

The rotation of the turntable ensures a constant slip condition of the contact patch. No stick-slip behavior was observed, and if we model the lateral force conveyed during slipping using a Coulumbic kinetic friction model, the effects of electroadhesion can be incorporated by including an additional component of normal force [21]. This is represented below, where F_l is the lateral friction force (denoted in Fig. 2b), μ is the kinetic coefficient of friction, F_n is the externally applied normal force, and F_e is the instantaneously applied electroadhesive force.

$$F_l = \mu(F_n + F_e) \tag{1}$$

If F_n is held constant, and μ is assumed constant, then any additional lateral force, F_{add}, is solely proportional to additional applied electroadhesion force.

$$F_{add} \propto F_e, \quad F_{add} = F_l - \mu F_n \tag{2}$$

C. Electrical Impedance Model

While vital to understanding, a full electrical impedance characterization of the finger/DLC system is beyond the

scope of this work, and will be reported in a subsequent work. Instead, we review aspects of the model that inform the force measurements. The gap impedance electrical model introduced in [3] is applied here. This model states that the magnitude of additional applied electroadhesive normal force, F_e, is proportional to the square of the voltage, V_g, across the finger/DLC interface gap.

$$|F_e| \propto |V_g|^2 \tag{3}$$

Additionally, V_g is related to the total applied current, I_t, via the concept of the gap impedance, Z_g (described in [3]).

$$|V_g| = |I_t||Z_g| \tag{4}$$

While the gap impedance includes resistive, R_g, and capacitive, C_g, elements, the resistance is neglected here. This is because the applied modulation method utilizes a carrier frequency current that is an order of magnitude larger than the measured cutoff frequency, $1/R_gC_g$, of the gap. Equations (2), (3), and (4) can then be combined and simplified yielding

$$|F_{add}(f)| \propto \left[\frac{|I_t(f)|}{2\pi f C_g}\right]^2. \tag{5}$$

This equation conveys two important limitations for current controlled excitation: first, that the additional force will exhibit an overall attenuation with frequency due to the capacitive nature of the gap, and second, the bandwidth of the electroadhesive force is directly dependent on the bandwidth of the current controller. The former is mitigated by the high frequency modulation process, while the later may be neglected below the current controller's 45 kHz bandwidth.

V. Data and Discussion

A. General Protocol

All measurements were made with the lead author's non-dominant index finger. The fingerpad and electroadhesive surface were cleaned with a 70% isopropyl alcohol solution and allowed to dry prior to measurement. Applied normal force was regulated at 1 N by the subject using a visual monitor. Typical fluctuations were small (<0.1 N). Translational velocity was held at 170 mm/s, and negligible deviations were observed. Double side-band, full-carrier (DSBFC) modulation was used for all experiments (f_c = 25 kHz).

B. Quasi-static Transduction Curve

A representative quasi-static curve of total peak current versus measured lateral force can be seen in Fig. 3. The carrier wave was sinusoidally modulated at 1 Hz for 100 seconds, yielding 100 traces of the curve. Negligible hysteresis was observed, and all traces were binned and averaged.

Total peak current was computed as the magnitude of the analytic representation of measured current, found using the Hilbert transform. Applied peak voltage remained below 100 V, and a plot of voltage versus lateral force yielded the same shape as Fig. 3, as the total system impedance remained linear. The curve is offset due to normal kinetic friction, and the additional force above 0.5 N is a result of additional electroadhesion force, as described by (2).

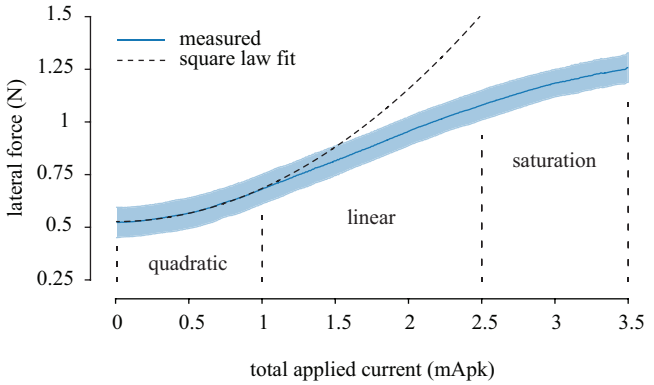

Fig. 3. Lateral force versus peak applied current, averaged over 100 seconds of 1 Hz sinusoidal modulation (1 N normal force). The solid line represents the trace mean, and the shaded region denotes $\pm\sigma$. Three distinct regions can be seen, a quadratic region (which can be fit with an offset square law), a relatively linear region, and a saturation region.

Below 1 mA total peak current, the measurement can be reasonably fit by an offset square law, as predicted by (3). At larger currents, however, the relationship appears to flatten out. This creates a reasonably linear region of the curve and, at even higher currents, a saturation region. This behavior for large currents is not explained by the present electroadhesion force model, and is subject to further investigation.

C. Sinusoidal Current to Lateral Force Response

Fig. 4 shows a measured current to force magnitude response of the electroadhesive system. Thirty logarithmically spaced modulation frequencies (10 Hz to 10 kHz) were individually tested in a series of 10 trials. Frequency order was randomized within trials, and the 25 kHz carrier was fully modulated for 2 seconds, resulting in a 0-3 mA sinusoidal envelope. A 3 mA maximum peak current was used in order to test the bandwidth of the system for large forces. The current envelope was extracted using the analytic representation. Peak current and lateral force magnitudes were computed using a digital lock-in technique and divided to yield the ratio.

As seen in Fig. 4, the current to force response is essentially flat throughout the entire measurement range. The peak and attenuation beginning at 6 kHz (denoted by the

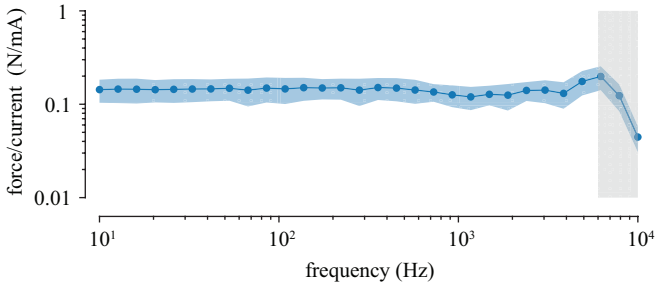

Fig. 4. Current to lateral force magnitude response reveals a flat response of ≈150 mN/mA throughout entire measurement range (recorded at 3 mApk current and 1 N normal force). Each point is mean of 10 trials. The blue shaded area represents $\pm\sigma$, while the gray shaded region denotes measurements past the resonance of the force sensing setup (included for reference, but may be ignored).

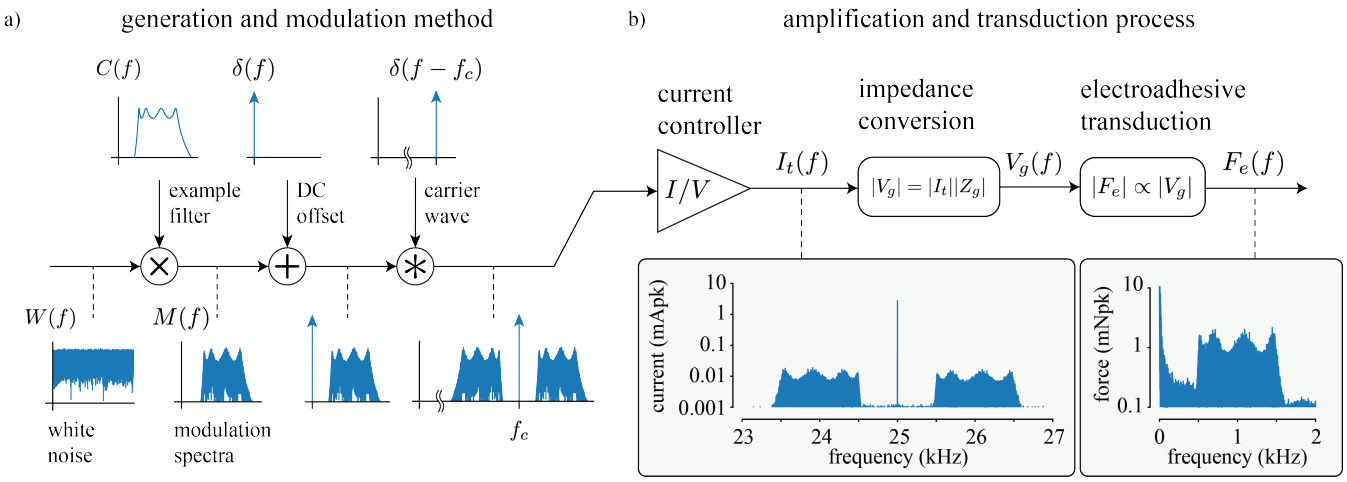

Fig. 5. a) An illustrative broadband signal is generated by taking the spectrum of a white noise source, $W(f)$, and multiplying it by a Chebyshev type I bandpass filter, $C(f)$. The resulting spectrum, $M(f)$, contains broadband noise from 500-1500 Hz, and represents a desired modulation spectrum. A DC offset, $\delta(f)$, is added, and a sinusoidal carrier wave, $\delta(f - f_c)$, is convolved with the signal according to conventional DSBFC AM modulation. b) A custom current controller takes the desired current spectrum and applies it to the finger/DLC interface, as seen by a recorded plot of $I_t(f)$. This current induces a matching gap voltage spectrum according to the gap impedance. The electroadhesive transduction process converts the gap voltage to an additional applied force to the sliding finger. This process also serves to demodulate the signal, recovering the original desired spectrum, $M(f)$, as evidenced by the plot of measured additional lateral force.

gray shaded region) is most likely a result of the force sensor's inherent resonance (shown in Fig. 2c) and not inherent to the transduction process. In fact, there is little evidence or theory to suggest appreciable force attenuation even above 6 kHz, as strong audio response is still recorded at modulation frequencies of 15 kHz. Even higher bandwidth force measurements would be needed to test this hypothesis.

D. Application of Broadband Force Spectra

The described electroadhesive system can be used to apply arbitrary broadband force spectra to the skin of the finger, as shown in Fig. 5. In this example, an illustrative broadband signal was constructed using bandpassed white noise. The signal was 60 seconds long, and contained the majority of its frequency content within the range of 500 to 1500 Hz, as seen by the spectrum $M(f)$ in Fig. 5a.

This signal was passed through the DSBFC modulation process in the digital domain. A DC offset of 1.75 mA was applied in order to bias it into the relatively linear portion of the quasi-static transduction curve (Fig. 3). It was then multiplied by a 25 kHz sinusoid, resulting in a signal with an envelope approximately ranging between 0 and 3.5 mApk. The signal was then reconstructed by the DAQ and converted to an applied current by the current controller. A measurement of the output current spectrum (shown in Fig. 5b) reveals the upper and lower sidebands of the applied signal, and the large 25 kHz carrier component.

The lateral force spectrum resulting from this current stimulation (also shown in Fig. 5b) shows the recovery of the original modulation spectrum, $M(f)$, from the demodulation performed by the transduction process. Note that the overall shape and relative magnitude of the modulation spectrum appear preserved throughout the entire process. The inherently non-linear system seems to exhibit remarkably linear overall behavior. This may be due to biasing the desired

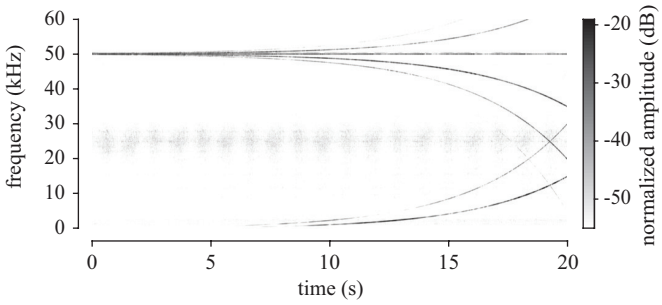

Fig. 6. Spectrogram of microphone response to a 100 Hz-15 kHz, 20 s logarithmic chirp. A peak current of 1 mA and a carrier frequency of 25 kHz was used. The recovered spectra can be seen at the bottom of the plot, while the copied spectra is seen centered around 50 kHz. Noise spanning 20-30 kHz corresponds to background noise from the sliding finger, modulated by turntable rotation, and amplified by the microphone's resonance.

signal in the middle of the quasi-static transduction curve. In this special case, it is proposed that the square-law in (3) may be suitably approximated by a purely linear relationship. The non-linearities of the system, however, can still be revealed under other conditions, as shown in the following section.

E. High Frequency Microphone Spectra

The demodulation process shifts part of the current spectrum back to the origin, recovering $M(f)$, and, according to theory, should also shift a copy of the spectrum to $2f_c$, creating high frequency force ripple on the finger. Centered around 50 kHz, this force spectrum cannot be sensed by the piezo force sensor nor is it directly perceptible by humans. Empirical evidence of of this force, however, has been captured in the recording of sound emitted from the finger.

Fig. 6 shows a spectrogram response of an ultrasonic microphone placed near the finger during logarithmic chirp modulation. The modulation lasted 20 seconds, starting at 100 Hz and ending at 15 kHz. Amplitude was limited

between 0-1 mApk, in order to stay in the quadratic portion of the transduction curve.

From this plot we can see that the copied spectra does indeed produce force on the finger, as seen by the 50 kHz component and upper and lower side-bands expanding outwards, confirming the existence of force at these frequencies. Additionally, a strong second harmonic of the original spectrum can be seen in both the recovered and copied spectra, reinforcing squared law behavior in this range. Also of note is the lack of any narrowband audio content at the original 25 kHz carrier frequency (broadband background noise is shown for reference, see caption).

VI. Conclusions

These recordings and models have several implications for the application of this technique to surface haptic and audio-haptic displays. To begin, this technique may be readily applied to the entire frequency range of perceivable tactile forces (DC-1 kHz). As shown, entire broadband force spectra can be applied to the finger (with seemingly small amounts of distortion). Thus, electroadhesive based devices appear quite well suited for high performance tactile rendering.

Additionally, this analysis reinforces the point that high performance hardware is needed if high performance, safe, and repeatable results are expected. For example, even if only a 1 kHz bandwidth is desired, at least a 11 kHz carrier should be applied so that the copied force spectrum doesn't leak into the audible frequency range (<20 kHz). At higher frequency, however, greater currents are needed to generate the same force, which increases the risk of inadvertent electrocutaneous stimulation. The use of current control dramatically reduces this risk.

In the case of audio-haptic displays, the initial measurements (such as Fig. 6) show promising results. The frequency range of applied force is exceedingly large, and is confirmed flat through at least 6 kHz. The relationship between force and the audible vibration, however, remains to be investigated. Use of an unconstrained finger on a flat surface will introduce relevant fingertip and surface dynamics, which may dramatically alter the sound emitted from the interaction. That said, signals such as intelligible speech and musical song are able to be passed through the system while remaining remarkably recognizable.

ACKNOWLEDGMENT

This material is based upon work supported by the National Science Foundation grant number IIS-1518602. Thanks to Oerlikon Balzers Coating USA, Inc. for providing the DLC coating.

References

[1] J. Linjama and V. Mkinen, "E-sense screen: Novel haptic display with capacitive electrosensory interface," *HAID*, vol. 9, pp. 10–11, 2009.

[2] O. Bau, I. Poupyrev, A. Israr, and C. Harrison, "TeslaTouch: electrovibration for touch surfaces," in *Proceedings of the 23nd annual ACM symposium on User interface software and technology*, ser. UIST '10. New York, NY, USA: ACM, 2010, pp. 283–292.

[3] C. Shultz, M. Peshkin, and J. Colgate, "Surface haptics via electroadhesion: Expanding electrovibration with Johnsen and Rahbek," in *2015 IEEE World Haptics Conference (WHC)*, Jun. 2015, pp. 57–62.

[4] L. Winfield, J. Glassmire, J. E. Colgate, and M. Peshkin, "T-PaD: Tactile Pattern Display through Variable Friction Reduction," in *EuroHaptics Conference, 2007 and Symposium on Haptic Interfaces for Virtual Environment and Teleoperator Systems. World Haptics 2007. Second Joint*, Mar. 2007, pp. 421 –426.

[5] M. Biet, F. Giraud, and B. Lemaire-Semail, "Squeeze film effect for the design of an ultrasonic tactile plate," *IEEE Transactions on Ultrasonics, Ferroelectrics, and Frequency Control*, vol. 54, no. 12, pp. 2678–2688, Dec. 2007.

[6] E. Vezzoli, W. B. Messaoud, M. Amberg, F. Giraud, B. Lemaire-Semail, and M. A. Bueno, "Physical and Perceptual Independence of Ultrasonic Vibration and Electrovibration for Friction Modulation," *IEEE Transactions on Haptics*, vol. 8, no. 2, pp. 235–239, Apr. 2015.

[7] R. S. Johansson and J. R. Flanagan, "Coding and use of tactile signals from the fingertips in object manipulation tasks," *Nature Reviews Neuroscience*, vol. 10, no. 5, pp. 345–359, May 2009.

[8] H. P. Saal, X. Wang, and S. J. Bensmaia, "Importance of spike timing in touch: an analogy with hearing?" *Current Opinion in Neurobiology*, vol. 40, pp. 142–149, Oct. 2016.

[9] A. I. Weber, H. P. Saal, J. D. Lieber, J.-W. Cheng, L. R. Manfredi, J. F. Dammann, and S. J. Bensmaia, "Spatial and temporal codes mediate the tactile perception of natural textures," *Proceedings of the National Academy of Sciences*, vol. 110, no. 42, pp. 17 107–17 112, Oct. 2013.

[10] D. J. Meyer, M. A. Peshkin, and J. E. Colgate, "Tactile Paintbrush: A procedural method for generating spatial haptic texture," in *2016 IEEE Haptics Symposium (HAPTICS)*, Apr. 2016, pp. 259–264.

[11] D. Meyer, M. Wiertlewski, M. Peshkin, and J. Colgate, "Dynamics of ultrasonic and electrostatic friction modulation for rendering texture on haptic surfaces," in *2014 IEEE Haptics Symposium (HAPTICS)*, Feb. 2014, pp. 63–67.

[12] M. Wiertlewski, D. Leonardis, D. J. Meyer, M. A. Peshkin, and J. E. Colgate, "A High-Fidelity Surface-Haptic Device for Texture Rendering on Bare Finger," in *Haptics: Neuroscience, Devices, Modeling, and Applications*. Springer Berlin Heidelberg, Jun. 2014, pp. 241–248, dOI: 10.1007/978-3-662-44196-1_30.

[13] M. Wiertlewski and J. E. Colgate, "Power Optimization of Ultrasonic Friction-Modulation Tactile Interfaces," *IEEE Transactions on Haptics*, vol. 8, no. 1, pp. 43–53, Jan. 2015.

[14] A. Johnsen and K. Rahbek, "A physical phenomenon and its applications to telegraphy, telephony, etc." *Journal of the Institution of Electrical Engineers*, vol. 61, no. 320, pp. 713–725, Jul. 1923.

[15] George Bartlett Prescott, *The Speaking Telephone, Talking Phonograph, and Other Novelties*. D. Appleton & Company, 1878.

[16] E. Gray, "Improvement in electric telegraphs for transmitting musical, tones," U.S. Patent US166 096 A, Jul., 1875, cooperative Classification H04L27/26.

[17] E. Mallinckrodt, A. L. Hughes, and W. Sleator, "Perception by the Skin of Electrically Induced Vibrations," *Science*, vol. 118, no. 3062, pp. 277–278, 1953.

[18] R. M. Strong and D. E. Troxel, "An Electrotactile Display," *IEEE Transactions on Man-Machine Systems*, vol. 11, no. 1, pp. 72–79, Mar. 1970.

[19] S. Grimnes, "Electrovibration, cutaneous sensation of microampere current," *Acta Physiologica Scandinavica*, vol. 118, no. 1, pp. 19–25, 1983.

[20] D. J. Beebe, C. M. Hymel, K. A. Kaczmarek, and M. E. Tyler, "A polyimide-on-silicon electrostatic fingertip tactile display," in *Proceedings of 17th International Conference of the Engineering in Medicine and Biology Society*, vol. 2, Sep. 1995, pp. 1545–1546 vol.2.

[21] D. Meyer, M. Peshkin, and J. Colgate, "Fingertip friction modulation due to electrostatic attraction," in *World Haptics Conference (WHC), 2013*, 2013, pp. 43–48.

[22] "IEEE Standard for Safety Levels with Respect to Human Exposure to Radio Frequency Electromagnetic Fields, 3 kHz to 300 GHz," *IEEE Std C95.1-2005 (Revision of IEEE Std C95.1-1991)*, pp. 1–238, Apr. 2006.

[23] M. Wiertlewski and V. Hayward, "Mechanical behavior of the fingertip in the range of frequencies and displacements relevant to touch," *Journal of Biomechanics*, vol. 45, no. 11, pp. 1869–1874, Jul. 2012.